14th International Congress of the International Society for Photogrammetry
Hamburg 1980

Commission No.III, Working Group No.2, Invited Paper
on

Image Correlation and Change Detection

Wolfgang M. Göpfert, Institut für Angewandte Geodäsie
D-6000 Frankfurt, Federal Republic of Germany

Abstract: Automatic change detection employing correlation techniques re-
presents an attractive alternative to manual methods. The image manipula-
tions required are presented, the emphasis being placed on correlation tech-
niques. The impact of gray-level and noise characteristics on the correla-
tion function, correlatibility aspects, computation techniques, and feed-
back algorithms are discussed.

1. Introduction

Change detection is a technique in which one compares two images of the same
areas taken at different times ("multitemporal imagery") to determine where
major changes have occured. The degrees of change depend on the type of
imagery, the exposure conditions, and the time difference between exposures.
In any instance, a search for changes will involve tediously checking areas
of no change while trying to detect changes.
By automating the change detection process, the human observer is set free
to concentrate on the analysis of detected changes rather than performing
the detection himself. For high-volume data processing the automated pro-
cess (see Fig. 1) offers an attractive alternative to purely manual image
processing due to its speed and cost-effectiveness. This paper will discuss
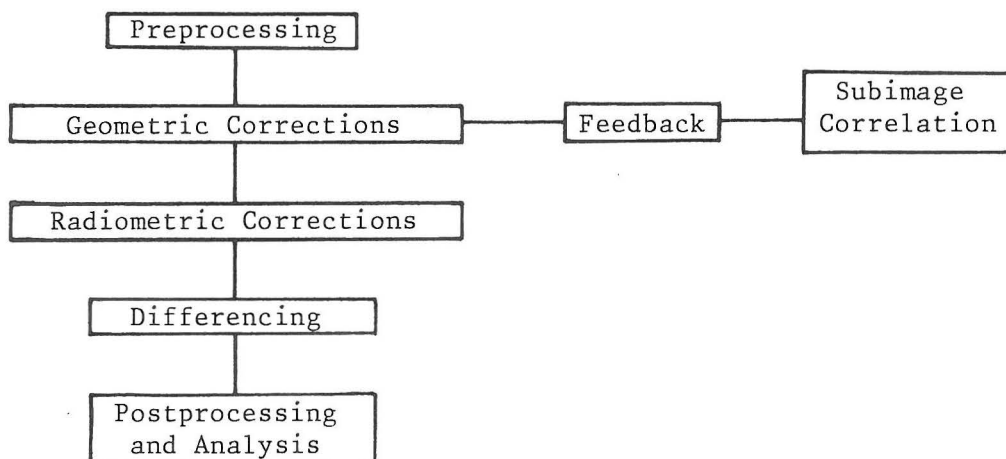the various processing steps with emphasis on the correlation technique.

Figure 1   Change detection process

2. Preprocessing

2.1 Calibration and Normalization

For most remote sensors, internal radiometric calibration cannot be imple-
mented consistently from sensor to sensor and for multitemporal imagery.

Further atmospheric effects such as haze and cloud cover necessitate normalization of multi-image data. There exist three basic procedures to provide good radiometric calibration and normalization of multitemporal imagery /18/. In equal interval quantizing the range of the original gray values is divided into equal length intervals, i.e. multi-images which are identical except for a linear scaling and different gray-level means will produce identical equal interval quantized images. In equal probability quantizing for any interval of gray-levels the number of image elements is made the same as for all other intervals. In data normalization the original data are normalized to a pregiven mean and variance.

2.2 Filtering

The first objective is to compensate image degradations caused by the sensor. In the case of image-motion blur (the convolution of the true image with a rectangular pulse corresponding to the length of the exposure) the degrading transfer function can be analytically modelled and subsequently be removed by inverse filtering /1/,/34/. Loss of details due to modulation transfer function (MTF) roll off can be compensated by boosting the high spatial frequencies with a filter that is the reciprocal of the MTF /1/. The removal of high frequency noise or periodic system noise can be implemented using low-pass and band-reject filtering, respectively /7/,/23/.

The second objective of preprocessing is to selectively preprocess the object information involving edge enhancement, differentiation, integration or pass/reject-filtering techniques /24/. As an example for remote sensor data consider the removal of shading or glare effects /7/.
All filtering operations may be performed either in the spatial frequency domain using Fast Fourier Transform (FFT) algorithms /9/ or in the spatial domain using the convolution technique. The advantage of filtering via the FFT is ease and versatility of the frequency filter design technique /12/, /35/, one filter operation requiring a total of $4 \text{ NM} \log_2 \text{NM} + \text{NM}$ complex operations. The (equivalent) direct convolution in the spatial domain offers a time advantage for small non-zero areas of the filter point-spread function, the spatial equivalent to the frequency filter /17/.

3. Geometric Corrections

3.1 Principle

Multitemporal imagery must be registered with respect to one common geometric data base prior to automatic change detections. The image mismatches may be caused by different sensor design characteristics and/or temporally different sensor orientations (altitude, attitude). Denoting the image coordinates of images $i=1,\ldots,I$ by x_i, y_i and the data base coordinates by x_b,y_b the problem is to map the images $i=1,\ldots I$ into the x_b,y_b system by the set of equations

$$x_i = f(x_b,y_b) \qquad y_i = g(x_b,y_b) \qquad i=1,\ldots I \tag{1}$$

where f and g are mapping functions to be discussed in section 3.2. Efficient implementations are carried out establishing first an interpolation grid ("anchor points") in the data base system, the grid spacing being chosen such that bilinear interpolation between these anchor points is sufficiently accurate. The registration process is performed using the indirect method: Point by point a set of x_b,y_b coordinates is defined, and the corresponding image coordinates x_i,y_i computed. Since x_i,y_i will in general not be integer numbers, a resampling must be carried out for all data base points /6/.

247.

3.2 Mapping Functions

Mapping functions can be defined using either parametric or non-parametric methods, whose orientation parameters or modelling coefficients, respectively, are determined through pass point coordinates like in conventional photogrammetry.

Parametric methods are based on the collinearity equations and the analytical modelling of the exterior orientation elements of the remote sensor, the resulting expressions optionally including object point elevations or a digital terrain model. For aircraft and satellite line-scanner imagery /4/, /28/,/33/, conical scanner imagery /32/, and side-looking airborne radar imagery /30/ these parametric methods have been extensively investigated.

Non-parametric methods include linear least squares prediction with and without filtering, meshwise linear interpolation /33/, bivariable polynomials /6/, multiquadric interpolation /14/,/16/ and other interpolation methods. Since in practical applications non-parametric methods gave results "which were comparable to or better than the ... parametric procedure" /33/, their application to geometric correction modelling is justified and also advantageous due to ease in handling and versatility. An investigation on the accuracy and economy of different interpolation methods (on topographic data) showed multiquadric interpolation to be the most efficient one /20/. Multiquadric theory and practical examples demonstrating the method's flexibility to irregularly distributed data have been published over the last decade /15/,/19/.

3.3 Pass point determination

Besides the manual measurement of a few initial pass points, pass point densification must be implemented by automatic means, i.e. by subimage correlation, in order to be operational. Since correlations can effectively detect translational bias only rather than rotational differences, prior to any correlation a geometric registration (with a minimum of 2 pass points) must be performed, in order to reduce the initial infinite number of rotational degrees of freedom. Therefore geometric and correlation algorithms must work in a feedback fashion rather than in a sequential mode, until the required pass points have been precisely determined.

4. Correlation

4.1 Principle

Subimage correlation is basically an operation of pattern-position-detection: Given a MxM gray-level pattern ("window" W) in image i, locate the same pattern in another image, e.g. the data base. For the time being assume both patterns to be located within identical geometric registration schemes. The correlation function and algorithm must detect the MxM subimage S^* inside a LxL, L>M search area A, which is most similar to the window W. In order to successfully apply correlation operations, the impact of gray-level and noise characteristics and the spatial resolution on the properties of the correlation function must be analysed and appropriately accounted for by adaptibility of the algorithms.

4.2 Characteristics of correlation functions

While in photogrammetry one is mainly concerned about spatial resolution of photographs, in image correlation it is the spatial frequency content (power spectrum) of the gray-level function d(x,y) that plays the key role. This is based on the Fourier transform relationship between its power spec-

trum $P(f_x, f_y)$ and its autocorrelation function $c_A(\Delta x, \Delta y)$, referred to as Wiener-Khinchin theorem /12/,/35/

$$c_A(\Delta x, \Delta y) = F^{-1}\{P(f_x, f_y)\} = \int_{-\infty}^{+\infty} P(f_x, f_y)\exp(j2\pi(\Delta x f_x + \Delta y f_y))df_x df_y \qquad (2)$$

where
F and F^{-1} = direct and inverse Fourier transform operators
$\quad f_x, f_y$ = spatial frequencies in lines/mm
$\quad \Delta x, \Delta y$ = shift (lag) coordinates

$$P(f_x, f_y) = /F\{d(x,y)\}/^2 = /\int_{-\infty}^{+\infty} d(x,y)\exp(-2\pi j(xf_x + yf_y))dxdy/^2 \qquad (3)$$

and $j = (-1)^{1/2}$. Figure 2 shows three examples for circularly symmetric power spectra, FR denoting the radial spatial frequency, and R the radial lag coordinate.

Fig. 2(a) has a bandlimited "white" power spectrum, its cut-off frequency F∅ governing the width of the correlation signal, which is the Besselfunction of first order, J_1, divided by its argument. For F∅ approaching zero, (a) illustrates the well-known fact that homogeneous gray-level patterns, i.e. a zero-frequency by itself, does not permit any successful correlation. For F∅ approaching infinity, it represents the ideal case of an unlimited "white" power spectrum, yielding a spike (delta-function) as correlation signal. Fig. 2(b) illustrates the contribution of a single frequency F∅ to a correlation signal. This contribution is a Besselfunction of zero order, increasing the frequency F∅ resulting in improved shapes of the correlation signal.

In aerial photography, power spectra generally display circular symmetry and show a decrease in power with increasing spatial frequency, approaching zero power at and beyond the resolution limit, as illustrated in Fig. 2(c). For a number of photographs of scales 1:50000 an average parameter F∅=2-3 lines/mm was found to be representative, resulting in approximate half-widths of 0.06 mm for the correlation function /29/. No useful frequency power was found to exist beyond 40 lines/mm. The limited impact of the higher frequencies on the correlation function of aerial photographs follows from combined interpretation of Fig. 2(b) and (c): Due to the exponential power loss their modelling effect on the shape and size of the correlation function is bound to be rather small.

4.3 Sources of input contamination

During data acquisition many noise sources degrade the data /8/. Electronic noise is caused by random thermal motion of electrons through the circuitry. Photoelectronic noise is encountered during the conversion process in image sensors due to the statistical nature of light. These two predominantly "white" noise sources can, however, be made arbitrary small by trading off time for improved signal-to-noise ratio S/N.

Therefore, photo grain noise during film scanning presents the main problem due to its deterministic spatial behaviour. Grain noise is due to the binary photographic process: A grain will be either exposed and subsequently reduced to metallic silver, or kept unexposed and washed off the emulsion. Density variations are then simply variations in grain-concentrations and so grain noise is signal-(density-) dependent. The S/N of a scanned film can be modelled as /21/

$$S/N = \frac{4.5\,a}{D^{1/2}\,\sigma(D)} \qquad (4)$$

with the local average density D, the scanning aperture diameter "a" in micro-meters, and the grain noise $\sigma(D)$ as decimal fraction of 0.001. Typical values for $\sigma(D)$ are 9 for High Definition Aerial, and 20 for Panatomic X film.

Another source of contamination is the MTF of the scanning aperture, additionally reducing the S/N ratio with increasing apertures.
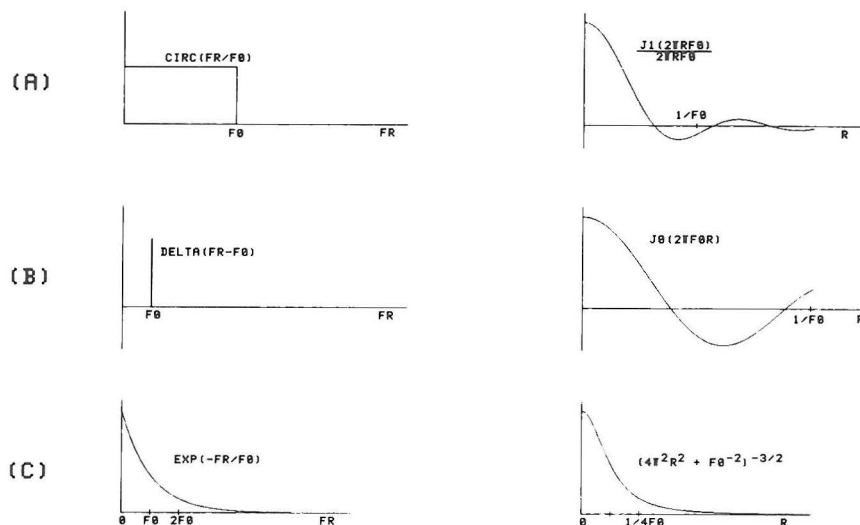

Figure 2   Relationship between power spectrum (left) and autocorrelation function (right) according to the Wiener-Khinchin theorem for circularly symmetric power spectra

4.4 Multi-level versus binary imagery

The number N of quantizing levels is important for the mean square error RMS to be expected for the correlation function. It has been shown that a small increase in N reduces this error sharply /10/. Several (N;RMS) pairs are reproduced here:

(2;72)   (4;2.75)   (8;1.23)   (16;1.05) ... (256;1.01) ... (∞;1.00)

This implies that binary quantized inputs must use about 72 times larger samples than inputs quantized to 8 bit (256 levels), in order to yield same expected errors. Since in photogrammetric "point" correlations the sub-image-sample is to be kept a minimum, binary quantized inputs are not feasible.

To this author's knowledge, the impact of selective binary quantization such as a gradient operation has not yet been investigated. Gradient images have the advantage of circumventing the problem of tone reversals frequently encountered in multitemporal imagery, since tonal borders will be invariant features in all images. However, gradient images are inherently noisy due to the high-pass filtering and differentiation effects, and very sensitive to the border threshold used. Up-to-date gradient image correlations did not prove superior to multi-level correlations in practical experiments /2/,/26/.

4.5 Computation techniques

Different correlation techniques offer largely different degrees of matching accuracy and computational economy. According to section 4.1, a total of $(L-M+1)^2$ subimages $S=(s_{ik})$, $i,k=1,...,M$ must be checked for similarity with

a MxM window $W = (w_{ik})$. Theoretically this would involve processing of $(L-M+1)^2 M^2$ windowing pairs of gray-levels (s_{ik}, w_{ik}). Since only a few points will be located in the neighborhood of the best match S^*, there is a considerable waste in computational effort involved when using rigorous computation techniques. Instead a simpler criterion should be used to define potential match positions.

An efficient algorithm to get to the neighborhood of the best match is called Sequential Similarity Detection Algorithm SSDA /5/. Its principle is to difference windowing pairs in a random nonrepeating sequence, sum the absolute values of the differences, and test this sum against a pregiven threshold value while windowing pairs are accumulated. When the threshold is exceeded, the subimage is immediately defined as a mismatch. For a suitable threshold /26/, many fewer than M^2 windowing pairs will have to be processed for mismatches, because for them rapid difference accumulation will occur. It is this property that significantly reduces the computing time by about two orders of magnitude.

Once the SSDA defined potential match positions, any of the following more efficient (but slower) techniques may be employed to precisely define the match position.

Correlation coefficient

The most commonly used correlation coefficient /6/,/11/,/31/ removes the mean value and uses complete normalization:

$$r = \sigma_{ws} / (\sigma_{ww} \sigma_{ss})^{1/2} \tag{5}$$

where σ_{ww}, σ_{ss} denote the statistical variances, and σ_{ws} the covariance.

Semi-normalized correlation coefficient

It is defined as $r_{sn} = \sigma_{ws} / \sigma_{ww}$, the difference to the correlation coefficient being that only the window-variance is used for normalization purposes. Although r_{sn} is theoretically somewhat inferior to r, differences in practice tend to be minor /21/.

Covariance

The covariance σ_{ws} is identical to a non-normalized correlation coefficient. Except for unusual cases, the positions of maximum covariance will coincide with those of maximum correlation coefficient.

Minimization of sum of squares of differences

The results are similar to those of the covariance, however, slightly more computations are needed.

Fourier transform correlation (FTC)

In Fourier transform correlation, the entire search area A (i.e. all possible subimages S) must be correlated at once with the window W /2/. It is clear that FTC is only practical when all those correlation values are actually required. FTC is the frequency domain equivalent of the covariance σ_{ws}, implemented by

$$FTC = F^{-1} \{F\{A\} \ F\{W\}'\} \tag{6}$$

where F and F^{-1} denote the direct and the inverse Fourier transform operators, implemented by FFT algorithms /9/, the prime (') indicating a complex conjugate operation, and A,W having their mean values removed. Upon complete normalization by the same computational technique as required for the correlation coefficient an exact replica of the correlation coefficient is obtained. The ratio of the number of equivalent integer add operations (on a general-purpose computer) necessary for computation of r and FTC is given as /5/

$$\frac{r}{FTC} = \frac{4.5 \ M^2 (L-M+1)^2}{200 \ L^2 \ \log_2 L} \tag{7}$$

For large windows and search ranges FTC becomes computationally superior, the requirement of M being a power of two for the FFT algorithm being readily circumvented by appropriate zero-fill.

Binary (Polarity) correlation

The numerator of the correlation coefficient is implemented by additions rather than multiplications: +1 is added when the windowing pair is alike, -1 is added when they are unlike. Computationally, this method is fast, but reliability for small windows rather low (see section 4.4).

Complex exponentiation correlation (CEC)

The real-valued windowing pairs are mapped into the complex number domain by the operations /13/,/16/

$$w_{ik} \rightarrow \exp(-jpw_{ik}) \quad \text{and} \quad s_{ik} \rightarrow \exp(-jps_{ik}) \quad i,k=1,M \tag{8}$$

where p denotes an exponentiation parameter governing the conversion of gray-level differences into phase changes $p(w_{ik}-s_{ik})$. Application of the theory of linear systems yields as correlation function squared

$$CEC = / \sum_{i,k} \exp(-jp(w_{ik}-s_{ik}))/^2 = / \sum_{i,k} \cos p(w_{ik}-s_{ik})/^2 + / \sum_{i,k} \sin p(w_{ik}-s_{ik})/^2 \tag{9}$$

which is invariant with different data mean values. For mismatches the phases tend to be incoherent meaning CEC approaches zero. For match positions, however, the phases tend to be differentially coherent (a constant phase bias is of no impact) and thus produce a maximum provided contaminating noise does not destroy or "swamp" this coherence. The influence of contaminating effects can be controlled by appropriately limiting the value of p by the empirical relation

$$p \leq 0.5\pi/(\sigma_{AA} + \sigma_{ww})^{1/2} \tag{10}$$

where σ_{AA}, σ_{ww} are the variances of search and window areas, respectively. In summary it follows that autocorrelations produce a spike (delta-function), meaning the power spectrum has been whitened by the complex exponentiation. This is merely the ideal case as illustrated by Fig. 2(a) for $F\emptyset \rightarrow \infty$.

Subpixel match positions

The exact match position will in general not be located at integer coordinate positions in the data base. In order to obtain subpixel accuracy some investigators /6/,/31/ fit a least squares smooth surface (e.g. a cone with an elliptical base) to a small grid of correlation values surrounding the best _ _eger match position, defining the location of the surface's maximum as best non-integer match position.

4.6 Correlatibility and geometric feedback considerations

The initial stage of subimage correlation must be performed on imagery being only globally corrected for geometric distortions. Consequently only the coarse image details of corresponding areas will be in-registration. An appropriately large window area must be defined to enable meaningful low-frequency correlation and to avoid false correlations due to significant power of the medium out-of-registration frequencies /21/,/14/. For computational efficiency QxQ original pixels may be combined to one window pixel, Q depending on the ratio of scanning and correlated frequency /14/,/16/. To avoid useless computational efforts window locations should be selected at tonal borders by checking a gradient threshold. This initial stage merely serves as a pull-in or lock-on procedure, defining a larger pass point set of good accuracy enabling the vital subsequent feedback operation, i.e. the updating of the geometry.

During higher correlation stages medium and higher frequencies are permitted to influence the correlation function to improve the matching accuracy. Due to the updated geometry the correlatibility of these higher frequencies has become meaningful. Again, window sizes must be used according to the lowest correlated frequency. This process is repeated until the finest resolvable detail has been correlated, a cutoff frequency being estimated by unreliable small S/N ratios and unpermittable MTF-degradations on the higher frequencies. A frequency ratio of 2:1 between successive iterations was found to work quite efficiently /22/.

5. Radiometric corrections

Apart from the generally small percentage of real object changes, gray-levels of corresponding image positions should ideally lie along a 45° regression line. Deviations from a 45° slope and a non-zero intercept give evidence of differences in contrasts and mean gray values, respectively, as might be caused by different film speeds, exposure times etc. Since differences in mean values and contrasts are in general a spatial image function, appropriate radiometric correction must be performed prior to any subsequent processing /31/.

6. Differencing

After radiometric corrections have been applied, the images of interest are differenced pixel by pixel. Commonly a thresholded difference image is produced: Pixels within some threshold T of 128 are all set to a neutral gray-level, e.g. 128. Pixels that were originally between 0 and 128 minus T are set to zero, while all those originally between 128 plus T and 255 are set to 255. All pixels of values zero or 255 indicate features present only in one of the images, while neutral gray-level areas indicate areas of no significant change. The threshold T is determined automatically for small subregions by evaluating the RMS deviations of their pixels in a direction perpendicular to the subregion regression line /16/,/31/.
By producing such a thresholded difference image the user is able to overcome the tedious and time-consuming looking back and forth between the images to be compared. Instead, he can immediately concentrate on the qualitative assessment of changes by interpretation of the areas concerned in the original imageries.

7. Postprocessing and analysis

The two geometrically and radiometrically corrected images can alternately or additionally serve as input to a combined change detection and pattern recognition algorithm. Parameters of entropy, a correlation coefficient, and high-intensity probability may be calculated for subregions, a non-linear discrimination algorithm being subsequently employed to optimally separate subregions with changes from those where no changes were detected /27/. Sequences of two or more images may be analysed using first-order difference images, providing a separate estimate for images of moving objects and of stationary scene components /25/. For the analysis of changes in coastal environments four techniques were investigated, a comparison of independently produced spectral classifications being one of the most promising ones /3/.

8. References

BuL = Bildmessung und Luftbildwesen, IEEE Tr. = Institute of Electrical and Electronics Engineers Transactions, PE = Photogrammetric Engineering (and Remote Sensing)

/1/ Andrews, H.C.: Computer Techniques in Image Processing. Academic Press, New York, 1970.

/2/ Anuta, P.: Spatial Registration of MSS and Multitemporal Digital Imagery Using FFT Techniques. IEEE Tr. Vol.GE-8,1970, p. 353-368.

/3/ Anuta, P.E.etal: Change Detection in Coastal Zone Environments. PE, Vol. 43, 1977, p. 1533-1539.

/4/ Bähr, H.P.: Geometrische Modelle für Abtasteraufzeichnungen von Erderkundungssatelliten. BuL 5/1976, p. 198-204.

/5/ Barnea, D.T. and Silverman, H.: A Class of Algorithms for Fast Digital Image Registration. IEEE Tr. Vol. C-21, 1972, p. 179-186.

/6/ Bernstein, R. and Ferneyhough, D.: Digital Image Processing. PE, Vol. 41, 1975, p. 1465-1476.

/7/ Billingsley, F.C.: Applications of Digital Image Processing. Journal of Applied Optics, Vol. 9, 1970, p. 289-299.

/8/ Billingsley, F.C.: Noise Considerations in Digital Image Processing Hardware. In: Picture Processing and Digital Filtering, Huang, T.S., Editor. Springer-Verlag, Berlin & New York, 1975.

/9/ Brigham, E.D. and Morrow, R.E.: The Fast Fourier Transform. IEEE Spectrum, December 1967, p. 63-70.

/10/ Chang, K. and Moore, D.: Modified Digital Correlator and its Estimation Errors. IEEE Tr. Vol. IT-16, 1970, p. 699-706.

/11/ Gambino, L.A. and Crombie, M.A.: Digital Mapping and Digital Image Processing. PE, Vol. 40, 1974, p. 1295-1302.

/12/ Goodman, J.W.: Introduction to Fourier Optics. McGraw-Hill Book Company, New York and London, 1968.

/13/ Göpfert, W.: Digital Cross-correlation of Complex Exponentiated Inputs. Proc. Image Processing, TU Graz, Austria, 1977, p. 63-66.

/14/ Göpfert, W.: High-Precision Scanner Imagery Rectification using Dynamic Meshes of Digitally Correlated Pass Points. Proc. Image Processing, TU Graz, Austria, 1977, p. 67-71.

/15/ Göpfert, W.: Interpolationsergebnisse mit der Multiquadratischen Methode. Zeitschrift f. Vermessungswesen, Vol. 102, 1977, p. 457-461.

/16/ Göpfert, W.: Automatisiertes Erkennen von Objektveränderungen in multitemporalen Bilddaten. NAKAVERM, Reihe I, Nr. 78, p. 5-24, Institut für Angewandte Geodäsie, Frankfurt, 1979.

/17/ Hall, E.L.: A Comparison of Computations for Spatial Frequency Filtering. Proc. of the IEEE, Vol. 60, 1972, p. 887-891.

/18/ Haralick, R.M.: Automatic Remote Sensor Image Processing. In: Digital Picture Analysis, Rosenfeld, A., Editor. Springer-Verlag Berlin & New York, 1976.

/19/ Hardy, R.L.: Multiquadric equations of topography and other irregular surfaces. Journal of Geophysical Research, Vol. 76, 1971, p. 1905-1915

/20/ Hein, G. und Lenze, K.: Zur Genauigkeit und Wirtschaftlichkeit ver-
schiedener Interpolations- und Prädiktionsmethoden. Zeitschrift für
Vermessungswesen, Vol. 104, 1979, p. 492-505.

/21/ Helava, U.V.: Digital Correlation in Photogrammetric Instruments.
Photogrammetria, Vol. 34, 1978, p. 19-41.

/22/ Hobrough, G.: Digital On-Line Correlation. BuL 3/1978, p. 79-86.

/23/ Holdermann, F.: Methoden zur Bildverbesserung. BuL 2/1976, p. 53-61.

/24/ Huang, T.S., Editor: Picture Processing and Digital Filtering.
Springer-Verlag, Berlin & New York, 1976.

/25/ Jain, R. and Nagel, H.-H.: On the Analysis of Accumulative Difference
Pictures from Image Sequences of Real World Scenes. IEEE Tr. Vol.
PAMI-1, 1979, p. 206-214.

/26/ Kaneko, T.: Evaluation of Landsat Image Registration Accuracy.
PE, Vol. 42, 1976, p. 1285-1299.

/27/ Kawamura, J.G.: Automatic Recognition of Changes in Urban Development
from Aerial Photographs. IEEE Tr. Vol. SMC-1, 1971, p. 230-239.

/28/ Konecny, G. and Schuhr, W.: Digitale Entzerrung der Daten von Zeilen-
abtastern. BuL 4/1975, p. 135-148.

/29/ Krulikoski, S.J., Jr. etal: Charting Techniques with Coherent Light
Sources. Final Technical Report RADC-TR-69-44, Griffiss Air Force
Base, N.Y., USA, 1969.

/30/ Leberl, F.: Satellitenradargrammetrie. DGK, Nr. C 239, München, 1978.

/31/ Lillestrand, R.L.: Techniques for Change Detection. IEEE Tr. Vol.
C-21, 1972, p. 654-659.

/32/ Malhotra, R.C.: Geometric Evaluation of Skylab S-192 Conical Scanner
Imagery. PE, Vol. 43, 1977, p. 169-182.

/33/ Mikhail, E. etal: Analysis of digital MSS data. BuL 1/1975, p. 22-27.

/34/ Niemann, H.: Methoden der Mustererkennung. Akademische Verlagsgesell-
schaft, Frankfurt am Main, 1974.

/35/ Papoulis, A.: The Fourier Integral and its Applications. McGraw-Hill
Book Company, New York and London, 1962.